

## Tyre contact forces and calculation of translatory velocities.

M. Prem Jeya Kumar<sup>1\*</sup>, J.Hameed Hussain<sup>2</sup>, V. Srinivasan<sup>3</sup>, R. Anbazhagan<sup>4</sup>

<sup>1, 3, 4</sup>Department of Automobile Engineering, Bharath University, Chennai-73;

<sup>2</sup>Professor of Mechanical Engineering, Bharath University, Chennai-73

\*Corresponding author: E-Mail: coebharathuniversity@gmail.com

### ABSTRACT

The simulation of a vehicle model involves the determination of horizontal forces at the tyre/road interface. The main task of tyre modeling is to derive these forces. The parameters that are essential for the estimation of horizontal forces are tyre slip, tyre side slip angle, and friction coefficients. These are the inputs to the force equation.

**KEY WORDS:** Translator, Velocities, Horizontal.

### 1. INTRODUCTION

**Co-Efficient of Friction Calculation:** Friction co-efficient is given by

$$\mu = \frac{F_{fric}}{F_z} \quad (1)$$

$F_{fric}$  = Frictional force

$F_z$  = Normal force

The frictional force is to be found out in the longitudinal direction as well as the lateral direction of the tyre. To find these forces the friction co-efficient are needed in those directions. As per Burckhardt's approach the resultant friction co-efficient can be expressed in the direction of resultant slip and is given by the expression,

$$\mu = (c_1(1 - e^{-c_2 s_{res}}) - c_3 s_{res}) \quad (2)$$

Here  $c_1$ ,  $c_2$ ,  $c_3$  are parameters for various road types. The friction co-efficient is influenced by high wheel velocities and heavy normal loads acting on the tyres. These effects should also be included in the friction co-efficient calculation.

**Tyre Modeling Flowchart:** Figure 1. shows the procedure and different parameters involved in tyre modeling in the form of flow chart.

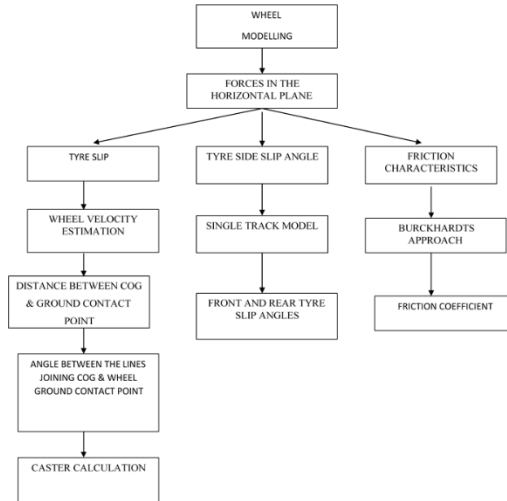


**Figure.1. Tyre modeling procedure**

Hence two more parameters  $c_4$ ,  $c_5$  are included in the equation 3.2 Equation 3.2 now becomes

$$\mu_{resij} = (c_1(1 - e^{-c_2 s_{resij}}) - c_3 s_{resij}) \cdot e^{-c_4 s_{resij} v_{cog}} \cdot (1 - c_5 F_{zij}^2) \quad (3)$$

**Table.1. Values of  $c_1$ ,  $c_2$ ,  $c_3$  for different road types**

Road Type	$c_1$	$c_2$	$c_3$
Asphalt dry	1.2801	23.99	0.52
Asphalt wet	0.857	33.822	0.347
Concrete	1.1973	25.168	0.5373
Cobblestones dry	1.3713	6.4565	0.6691
Cobblestones wet	0.4004	33.7080	0.1204
Snow	0.1946	94.129	0.0646
Ice	0.05	306.39	0

The values for parameters  $c_4$ ,  $c_5$  are given below:

www.jchps.com

 $c_4 = 0.03$  $c_5 = 0.00151$  $s_{res}$  – Resultant wheel slip $F_z$  - Vertical wheel load $V_{cog}$  – Vehicle velocity

The Equation 3.3 is given as a generalized format for all the wheels. The subscript “ $ij$ ” represents front/rear, left/right tyres. Thus the friction co-efficient for all the four tires are given by “equation (3.4)”

$$\begin{aligned}\mu_{resfl} &= (c_1(1 - e^{-c_2 s_{resfl}}) - c_3 s_{resfl}) \cdot e^{-c_4 s_{resfl} V_{cog}} \cdot (1 - c_5 F_{zfl}^2) \\ \mu_{resfr} &= (c_1(1 - e^{-c_2 s_{resfr}}) - c_3 s_{resfr}) \cdot e^{-c_4 s_{resfr} V_{cog}} \cdot (1 - c_5 F_{zfr}^2) \\ \mu_{resrl} &= (c_1(1 - e^{-c_2 s_{resrl}}) - c_3 s_{resrl}) \cdot e^{-c_4 s_{resrl} V_{cog}} \cdot (1 - c_5 F_{zrl}^2) \\ \mu_{resrr} &= (c_1(1 - e^{-c_2 s_{resrr}}) - c_3 s_{resrr}) \cdot e^{-c_4 s_{resrr} V_{cog}} \cdot (1 - c_5 F_{zrr}^2)\end{aligned}\quad (4)$$

The friction coefficients in the longitudinal ( $\mu_l$ ) and lateral ( $\mu_s$ ) directions can be calculated as follows:

$$\mu_{lij} = \mu_{resij} \frac{s_{lij}}{s_{resij}} \quad (5)$$

$$\mu_{sij} = \mu_{resij} \frac{s_{sij}}{s_{resij}}$$

 $s_{lij}$  – Longitudinal slip $s_{sij}$  - Lateral slip

The friction co-efficient in the lateral direction is less than that of in the longitudinal direction due to the tread profile. Hence an attenuation factor is used to correct the reduction. Usually the attenuation factor ( $k_s$ ) lies in between 0.90 and 0.95. Thus  $\mu_s$  becomes

$$\mu_{sij} = k_s \cdot \mu_{resij} \frac{s_{sij}}{s_{resij}} \quad (6)$$

From the above equations it is evident to determine the slip values to find the coefficient of friction values.

**Slip Calculation:** Wheel slip occurs due to the difference of the rotational equivalent of tyre velocity ( $V_r$ ) and the translatory velocity ( $V_w$ ) of the wheel. The acceleration and braking forces are produced due to the presence of slip. There are two types of slip,

- Longitudinal slip
- Lateral slip

If the tyre rotates without lateral slip, tyre slip is the difference between the rotational equivalent velocity and translatory velocity. But the longitudinal slip and lateral slip occur simultaneously. Usually Longitudinal slip is considered in the direction of motion of the wheel (i.e.) in the direction of wheel velocity and the lateral slip in the direction perpendicular to the direction of wheel velocity. The rotational equivalent wheel velocity is in the direction of X axis of the wheel coordinate system whereas the wheel velocity is inclined at tyre side slip angle to it. It is evident from the following figure. Hence  $V_r$  should be multiplied by the cosine of tyre side slip angle before calculating slip. In slip calculations the speed difference is divided the respective larger speed to avoid division by zero.

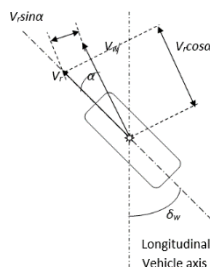


**Figure.2. Wheel slip calculation**

The slip is calculated for driving and braking conditions for all the four wheels.

### Braking

$$\text{Longitudinal slip } s_{lij} = \frac{v_{rij} \cos \alpha_{ij} - v_{wij}}{v_{wij}} \quad (7)$$

$$\text{Lateral slip } s_{sij} = \frac{v_{rij} \sin \alpha_{ij}}{v_{wij}}$$

### Driving

$$\text{Longitudinal slip } s_{lij} = \frac{v_{rij} \cos \alpha_{ij} - v_{wij}}{v_{rij} \cos \alpha_{ij}} \quad (8)$$

$$\text{Lateral slip } s_{sij} = \tan \alpha_{ij}$$

Resultant slip is given by

$$S_{resij} = \sqrt{s_{lij}^2 + s_{sij}^2} \quad (9)$$

- $S_{resij}$  Resultant slip
- $s_{lij}$  Longitudinal slip in the direction of  $v_{wij}$
- $s_{sij}$  Lateral slip in the direction perpendicular to  $v_{wij}$
- $\alpha_{ij}$  Tyre side slip angle
- $v_{rij}$  Rotational equivalent wheel velocity of tyre
- $v_{wij}$  Translatory wheel velocity

The subscript  $ij$  represents the front/rear, left/right tyres.

The three variables Tyre side slip angle, Rotational equivalent velocity of tyre and the translatory velocity of the tyre are calculated hereafter.

**Calculation of Rotational Equivalent Velocity of Tyre ( $v_{rij}$ ):** The rotational equivalent velocity of the tyre is given by the expression

$$v_{rij} = r_{effij} \cdot \omega_{ij} \quad (10)$$

- $v_{rij}$  Rotational equivalent velocity of tyre
- $r_{effij}$  Effective tyre radius
- $\omega_{ij}$  Angular velocity of the tyre
- $ij$  represents front/rear, left/right tyres

$r_{eff}$  calculation

Let the tyre run over a length " $l$ " for a time " $t$ " through an angle " $\phi$ ", then

$$\begin{aligned} v_r &= \frac{l}{t} & \omega &= \frac{\phi}{t} \\ &= r_{eff} \frac{\phi}{t} \end{aligned} \quad (11)$$

$$\text{Hence } r_{eff} = \frac{l}{\phi}$$

Consider Figure 3. Where the static and dynamic wheel radius is shown.

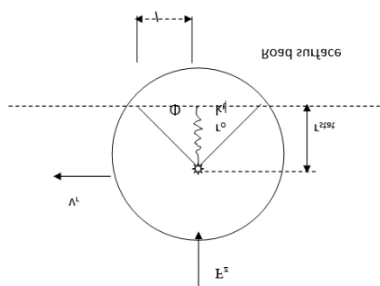


**Figure.3. Static and dynamic wheel radius**

From the figure 3.

$$\begin{aligned}
 r_{stat} &= r_o \cos \phi \quad ; \quad l = r_o \sin \phi \\
 \phi &= \cos^{-1} \frac{r_{stat}}{r_o} \\
 r_{eff} &= r_o \cdot \frac{\sin \left( \cos^{-1} \left( \frac{r_{stat}}{r_o} \right) \right)}{\cos^{-1} \left( \frac{r_{stat}}{r_o} \right)}
 \end{aligned}
 \tag{12}$$

**Calculation of Tyre Translatory Velocity:** The tyre translatory velocity or the tyre road contact point velocity can be found by transforming the vehicle COG velocity to the tyre ground contact point. To perform such transformation the following variables are necessary,

- Vehicle COG velocity
- Yaw rate
- Distance between Vehicle COG and tyre road contact point
- Angle between the line joining Vehicle COG and tyre road contact point
- Tyre side slip angle
- Wheel turn angle

The vehicle COG velocity can be obtained from sensor data. The yaw rate is calculated as function of time “t”. The other variables are calculated hereafter. The wheel turn angle can also be measured physically.

**Distances between Vehicle Cog and Tyre Road Contact Points:** The point of action of tyre force is the tyre ground contact point. It does not lie at the centre of the tyre road contact patch but it lies towards the rear due to wheel caster. It is evident from the Figure 4. It shows an aerial view of the tyre contact area including the tyre road contact point. The middle point of the tyre contact area migrates outwards and creates a torque with the longitudinal force which during acceleration increases self-aligning torque and during braking decreases it.

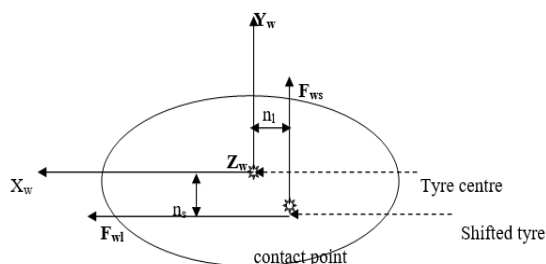


**Figure.4. View from above of tyre contact area**

- $X_w$  X axis of wheel coordinate system
- $Y_w$  Y axis of wheel coordinates system
- $Z_w$  Z axis of wheel coordinates system
- $F_{wl}$  Frictional force in the direction of  $X_w$
- $F_{ws}$  Frictional force in the direction of  $X_w$
- $n_l$  Longitudinal caster
- $n_s$  Lateral caster

The longitudinal and lateral casters can be calculated using the following relations

$$n_{lij} = \frac{1}{2} \left( -0.03 + 0.12 \frac{F_{zij}}{5000} \right) \tag{13}$$

$$n_{sij} = 3n_{lij} \tan \alpha_{ij}$$

- $n_{lij}$  Longitudinal caster of tyre
- $n_{lii}$  Lateral caster of tyre
- $F_{zij}$  Wheel vertical load
- $\alpha_{ij}$  Tyre side slip angle
- $ij$  represents front/rear, left/right tyres.

The caster is generally assumed to be constant and only the component in the direction of the wheel plane is considered. But, using the above method the caster can be calculated dynamically (with direction information). The frictional forces  $F_l$  and  $F_s$  act in the direction of the wheel velocity  $v_w$  and in a direction perpendicular to it. The  $F_{wl}$  and  $F_{ws}$  can be obtained by transforming the forces  $F_l$  and  $F_s$  into the wheel coordinate system.

The distance between the tyre ground contact point and Vehicle COG ( $r_{ij}$ ) can be calculated geometrically for each tyre. The angle between the line joining the Vehicle COG and the tyre/road contact point ( $\gamma_{ij}$ ) can also be found geometrically.

**Front Right Tyre**

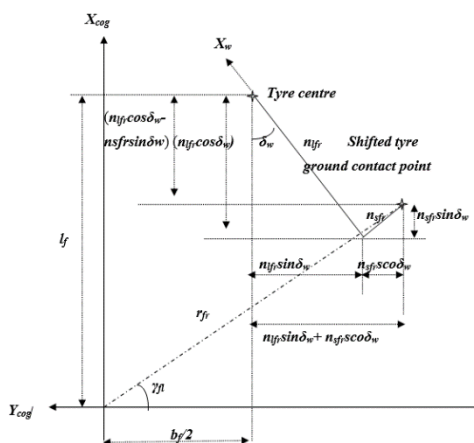
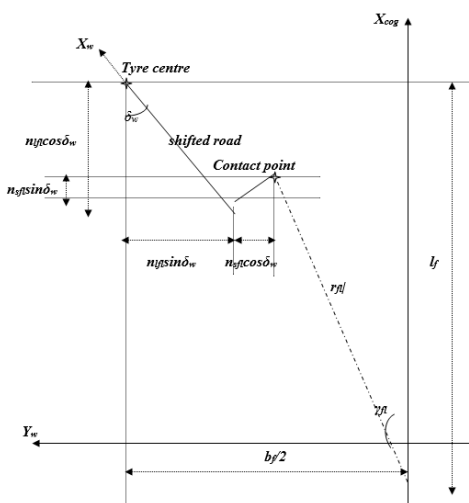


**Figure 5. Geometric calculation of the distance  $r_{fr}$**  (14)

$$r_{fr} = \sqrt{\left( l_f - n_{fr} \cos \delta_w + n_{fr} \sin \delta_w \right)^2 + \left( \frac{b_f}{2} + n_{fr} \cos \delta_w + n_{fr} \sin \delta_w \right)^2}$$

$$\gamma_{fr} = \tan^{-1} \left( \frac{l_f - n_{fr} \cos \delta_w + n_{fr} \sin \delta_w}{\frac{b_f}{2} + n_{fr} \cos \delta_w + n_{fr} \sin \delta_w} \right)$$

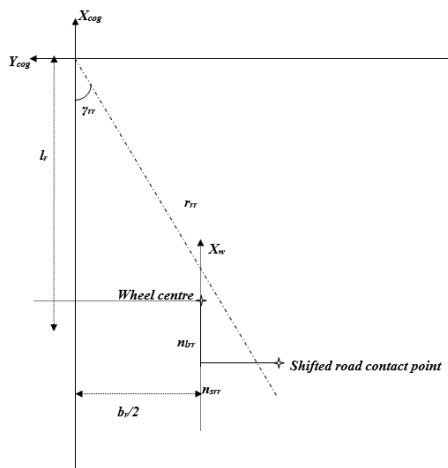
**Front Left Tyre**



**Figure 6. Geometric calculation of the distance  $r_{fl}$**

$$r_{fl} = \sqrt{\left(l_f - n_{fl} \cos \delta_w + n_{sfl} \sin \delta_w\right)^2 + \left(\frac{b_f}{2} - n_{fl} \sin \delta_w - n_{sfl} \cos \delta_w\right)^2}$$

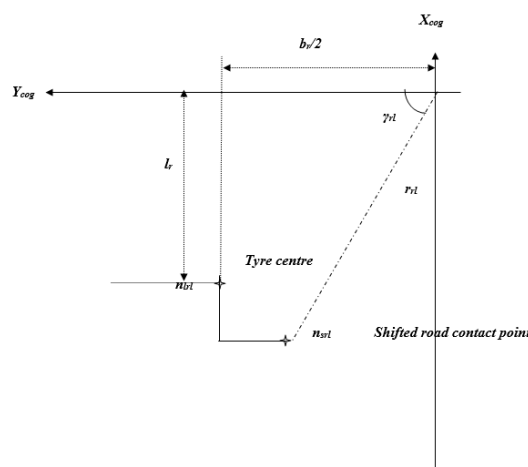
$$\gamma_{fl} = \tan^{-1} \left( \frac{\frac{b_f}{2} - n_{fl} \sin \delta_w - n_{sfl} \cos \delta_w}{l_f - n_{fl} \cos \delta_w + n_{sfl} \sin \delta_w} \right)$$

**Rear Right Tyre:****Figure 7. Geometric calculation of the distance  $r_{rr}$** 

$$r_r = \sqrt{\left[l_r + n_{lrr}\right]^2 + \left[b_r / 2 + n_{srr}\right]^2}$$

(16)

$$\gamma_{rr} = \tan^{-1} \left( \frac{b_r / 2 + n_{srr}}{l_r + n_{lrr}} \right)$$

**Rear Left Tyre****Figure 8. Geometric calculation of the distance  $r_{rl}$** 

$$r_{rl} = \sqrt{\left[l_r + n_{rl}\right]^2 + \left[b_r / 2 - n_{srl}\right]^2}$$

(17)

$$\gamma_{rl} = \tan^{-1} \left( \frac{l_r + n_{rl}}{b_r / 2 - n_{srl}} \right)$$

- $r_{fr}$  Distance between vehicle COG and front right tyre road contact point  
 $r_f$  Distance between vehicle COG and front left tyre road contact point  
 $r_{rl}$  Distance between vehicle COG and rear left tyre road contact point  
 $r_{rr}$  Distance between vehicle COG and rear right tyre road contact point  
 $\gamma_{fr}$  Angle between line joining vehicle COG, front right tyre road contact point and Vehicle COG coordinates system  
 $\gamma_{fl}$  Angle between line joining vehicle COG, front left tyre road contact point and Vehicle COG coordinates system  
 $\gamma_{rl}$  Angle between line joining vehicle COG, rear right tyre road Contact point and Vehicle COG coordinate system

$\gamma_{rr}$  Angle between line joining vehicle COG, rear left tyre road contact point and Vehicle COG coordinate system.

$l_f$  Distance between vehicle COG and front axle

$l_r$  Distance between vehicle COG and rear axle

$b_f$  Distance between wheels on front axle

$b_r$  Distance between wheels on rear axle

## 2. RESULT AND DISCUSSION

In an automotive vehicle system safety and riding comfort are the primary important parameters and the roll over stability is an important parameter related with stability. Higher operating speeds and ride comfort are of greater importance for passenger vehicles, greater axle loads are mainly considered for cargo carriers. Hence it is essential to obtain a better understanding of the automotive system to run the vehicle at higher operating speeds with more safety. It is hoped that the models and the techniques presented in this thesis, would provide an answer to the problem of safety at high operations related to an automotive vehicle system.

## 3. CONCLUSION

**Tyre construction:** Thicker treads and increased number of carcass plies result in more work to be done by the tyre while rolling thus resulting in high hysteresis losses and high rolling resistance.

**Road surface:** Rolling resistance is less for hard, smooth and dry road surfaces. Rolling resistance is high for worn out roads since more work is done by the tyre to roll over the uneven surfaces. Rolling resistance is high for wet surfaces.

**Tyre material:** Synthetic rubber is having more rolling resistance than natural rubber. Butyl rubbers have more rolling resistance than synthetic rubber but have good road holding and traction properties.

**Inflation pressure:** Depending on the road type inflation pressure affects the rolling resistance. On hard surfaces when inflation pressure increases rolling resistance decreases. On deformable road surfaces more inflation pressure results in high ground penetration and more work is to be done by the tyre. If the inflation pressure is less, more deflection occurs resulting in high rolling resistance. So an optimum tyre pressure is to be maintained.

**Speed:** As speed of the rolling tyre increases the work done in deforming the tyre also increases and hence the rolling resistance increases. The multitude of factors discussed previously lead to complexity in the determination of rolling resistance. However in performance calculations it is sufficient to express co-efficient of rolling resistance as a linear function of speed.

## REFERENCES

Aldo A, Ferri, Muhammad Haroon, Douglas E. Adams and Yiu Wah Luk, A Time and Frequency Domain Approach for Identifying Non - Linear Automotive Suspension System Model in the Absence of an Input Measurement, ASEM International Mechanical Engineering Congress and Exposition, IMECE, 2004, 60211.

Aldo Sornioti and Nicolò D, Alfio, Vehicle Dynamics Simulation to Develop an Active Roll Control System, SAE, 2007.

Alexander Hac, Rollover Stability Index Including Effects of Suspension Design, Society of Automotive Engineers, inc, 2002, 1396-1412

Allen R.W and Azostak H.T, Characteristics Influencing Ground Vehicle Lateral/Directional Dynamic Stability, SAE paper 910234, Society of Automotive Engineers, Warren dale, PA, 1991.

Allen R.W and Rosenthal T.J, Requirements for Vehicle Dynamics Simulation Models, SAE paper No.940175, Society of Automotive Engineers, Warren dale, PA, 1994.

Allen R.W, Rosenthal T.J, Klyde D.H. and Hogue J R, Computer Simulation Analysis of Light Vehicle Lateral / Directional Dynamic Stability, SAE Paper, 1999.

Allen R.W, Steady State and Dynamic Properties of All Terrain Vehicles Related to Lateral Directional Handling and Stability, SAE Paper 891105, Society of Automotive Engineers, Warren dale, PA, 1989.

Allen R.W, Szostak GH.T and Rosenthal T.J, Steady State and Transient Analysis of Ground Vehicle Handling, SAE paper 870495, Society of Automotive Engineers, Warren dale, PA, 1987.

Allen R.W, Vehicle Dynamic Stability and Rollover, NHTSA DTNH 22-88-C 07384, Systems Technology, Inc, 1991.

Brintha Rajakumari S, Nalini C, An efficient data mining dataset preparation using aggregation in relational database, Indian Journal of Science and Technology, 7, 2014, 44-46.

Jayalakshmi V, Gunasekar N.O, Implementation of discrete PWM control scheme on Dynamic Voltage Restorer for the mitigation of voltage sag /swell, International Conference on Energy Efficient Technologies for Sustainability, ICEETS 2013, 1036-1040.

Kaliyamurthie K.P, Parameswari D, Udayakumar R, QOS aware privacy preserving location monitoring in wireless sensor network, Indian Journal of Science and Technology, 6 (5), 2013, 4648-4652.

Kaliyamurthie K.P, Udayakumar R, Parameswari D, Mugunthan S.N, Highly secured online voting system over network, Indian Journal of Science and Technology, 6 (6), 2013, 4831-4836.

Khanaa V, Thooyamani K.P, Saravanan T, Simulation of an all optical full adder using optical switch, Indian Journal of Science and Technology, 6(6), 2013, 4733-4736.

Khanaa V, Thooyamani K.P, Using triangular shaped stepped impedance resonators design of compact microstrip quad-band, Middle - East Journal of Scientific Research, 18 (12), 2013, 1842-1844.

Kumaravel A, Dutta P, Application of Pca for context selection for collaborative filtering, Middle - East Journal of Scientific Research, 20 (1), 2014, 88-93.

Raj M.S, Saravanan T, Srinivasan V, A modified direct torque control of induction motor using space vector modulation technique, Middle - East Journal of Scientific Research, 20(11), 2014, 1572-1574.

Saravanan T, Raj M.S, Gopalakrishnan K, VLSI based 1-D ICT processor for image coding, Middle - East Journal of Scientific Research, 20 (11), 2014, 1511-1516.

Sengottuvel P, Satishkumar S, Dinakaran D, Optimization of multiple characteristics of EDM parameters based on desirability approach and fuzzy modeling, Procedia Engineering, 64, 2013, 1069-1078.

Sundararajan M, Optical instrument for correlative analysis of human ECG and breathing signal, International Journal of Biomedical Engineering and Technology, 6 (4), 2011, 350-362.

Thamotharan C, Prabhakar S, Vanangamudi S, Anbazhagan R, Anti-lock braking system in two wheelers, Middle - East Journal of Scientific Research, 20 (12), 2014, 2274-2278.

Udayakumar R, Khanaa V, Saravanan T, Saritha G, Retinal image analysis using curvelet transform and multistructure elements morphology by reconstruction, Middle - East Journal of Scientific Research, 16 (12), 2013, 1781-1785.

Vanangamudi S, Prabhakar S, Thamotharan C, Anbazhagan R, Design and fabrication of dual clutch, Middle - East Journal of Scientific Research, 20 (12), 2014, 1816-1818.

Vanangamudi S, Prabhakar S, Thamotharan C, Anbazhagan R, Design and calculation with fabrication of an aero hydraulic clutch, Middle - East Journal of Scientific Research, 20 (12), 2014, 1796-1798.